



Dalton
Transactions

**Hydrostannylation of Carbon Dioxide by a
Hydridostannylene Molybdenum Complex**

| | |
|-------------------------------|---|
| Journal: | <i>Dalton Transactions</i> |
| Manuscript ID | DT-ART-07-2021-002473 |
| Article Type: | Paper |
| Date Submitted by the Author: | 26-Jul-2021 |
| Complete List of Authors: | Zhu, Qihao; University of California, Department of Chemistry Fettinger, James; University of California, Davis, Chemistry Power, Philip; University of California, Department of Chemistry |
| | |

SCHOLARONE™
Manuscripts

Hydrostannylation of Carbon Dioxide by a Hydridostannylene Molybdenum Complex

Qihao Zhu, James C. Fettinger, and Philip P. Power*

Department of Chemistry, University of California, Davis, California 95616, United States

Email: pppower@ucdavis.edu

Abstract:

Reaction of the aryltin(II) hydrides $\{\text{Ar}^{\text{iPr}4}\text{Sn}(\mu\text{-H})\}_2$ or $\{\text{Ar}^{\text{iPr}6}\text{Sn}(\mu\text{-H})\}_2$ ($\text{Ar}^{\text{iPr}4} = \text{-C}_6\text{H}_3\text{-2,6-}(\text{C}_6\text{H}_3\text{-2,6-}^i\text{Pr}_2)_2$, $\text{Ar}^{\text{iPr}6} = \text{-C}_6\text{H}_3\text{-2,6-}(\text{C}_6\text{H}_2\text{-2,4,6-}^i\text{Pr}_3)_2$) with two equivalents of the molybdenum carbonyl $[\text{Mo}(\text{CO})_5(\text{THF})]$ afforded the divalent tin hydride transition metal complexes, $\text{Mo}(\text{CO})_5\{\text{Sn}(\text{Ar}^{\text{iPr}6})\text{H}\}$, (**1**), or $\text{Mo}(\text{CO})_5\{\text{Sn}(\text{Ar}^{\text{iPr}4})(\text{THF})\text{H}\}$ (**2**), respectively. Complex **1** effects the facile hydrostannylation of carbon dioxide, to yield $\text{Mo}(\text{CO})_5\{\text{Sn}(\text{Ar}^{\text{iPr}6})(\kappa^2\text{-O, O}'\text{-O}_2\text{CH})\}$, (**3**), which features a bidentate formate ligand coordinating the tin atom. Reaction of **3** with the pinacolborane, HBpin (pin = pinacolato) in benzene regenerated **1** in quantitative yield. All complexes were characterized by X-ray crystallography, as well as UV-visible, IR, and multinuclear NMR spectroscopies. The isolation of **1** and **2** is consistent with the existence of monomeric forms of $\{\text{Ar}^{\text{iPr}4}\text{Sn}(\mu\text{-H})\}_2$ and $\{\text{Ar}^{\text{iPr}6}\text{Sn}(\mu\text{-H})\}_2$ in solution. Regeneration of **1** from **3** via reaction with pinacolborane as the hydrogen source shows the catalytic potential of **1** in the hydrogenation of CO_2 .

Introduction

Tetravalent heavier group 14 element hydrides are well-known as reagents that effect numerous organic transformations under mild conditions.¹⁻⁹ In contrast, the corresponding reactions of their divalent hydride congeners are much less explored although they have been shown to display catalytic potential as a result of their coordinative unsaturation and their hydridic reactivity with

unsaturated molecules.¹⁰⁻¹² The first stable divalent organotin hydride, $\{\text{Ar}^{\text{iPr}_6}\text{Sn}(\mu\text{-H})\}_2$ ($\text{Ar}^{\text{iPr}_6} = \text{-C}_6\text{H}_3\text{-2,6-(C}_6\text{H}_2\text{-2,4,6-}^i\text{Pr}_3)_2$),¹³ was reported in 2000. This was followed by further examples¹⁴⁻²⁰ from a number of groups which included the three-coordinate organotin(II) hydride $[\{\text{HC}(\text{CMeNAr})_2\}\text{SnH}]$ ($\text{Ar} = \text{2,6-}^i\text{Pr}_2\text{C}_6\text{H}_3$) containing a terminal Sn-H bond as reported by Roesky and coworkers in 2006¹⁴, and the amido species $[\text{LSn}(\mu\text{-H})_2]$ ($\text{L} = \text{-N}(\text{Ar})(\text{SiPr}_3)$ $\text{Ar} = \text{C}_6\text{H}_2\{\text{C}(\text{H})\text{Ph}_2\}_2\text{Pr}^i\text{-2,6,4}$) as described by Jones and coworkers in 2013.¹⁹ In addition, there has been a growing interest in the reactivity of these hydrides with important small molecules (e.g. alkenes, alkynes, ketones, etc.),²¹⁻²⁷ transition metal complexes,²⁸⁻³¹ and their recently discovered involvement in equilibria between the multiply bonded group 14 species and hydrogen.³²

Recent work in this group has shown that the aryltin(II) hydrides $\{\text{Ar}^{\text{iPr}_4}\text{Sn}(\mu\text{-H})\}_2$ and $\{\text{Ar}^{\text{iPr}_6}\text{Sn}(\mu\text{-H})\}_2$ react rapidly with norbornene and norbornadiene as well as other alkenes to afford the similar hydrostannylation products $\text{ArSn}(\text{norbornyl})$ and $\text{ArSn}(\text{norbornenyl})$ at ambient temperature.³³ These results suggested that the reactive tin species is a monomeric $\text{Ar}^{\text{iPr}_4}\text{SnH}/\text{Ar}^{\text{iPr}_6}\text{SnH}$ unit that is in equilibrium with the dimer. Although a ^1H NMR calculation of the chemical shift of Sn-H in $\text{Ar}^{\text{iPr}_6}\text{SnH}$, which resonates at $\delta = 25.4$ ppm, suggests the presence of monomeric $\text{Ar}^{\text{iPr}_6}\text{SnH}$, no structurally characterized two-coordinate divalent tin(II) hydride has been reported to date.³⁴ Wesemann and coworkers reported a series of Lewis base-adducts of $\text{Ar}^{\text{iPr}_6}\text{SnH}$, which is the monomeric unit of $\{\text{Ar}^{\text{iPr}_6}\text{Sn}(\mu\text{-H})\}_2$, including NHCs, and DMAP, indicating the Lewis acidic nature of $\text{Ar}^{\text{iPr}_6}\text{SnH}$ moiety.³⁵⁻³⁷ On the other hand, isolation of $\text{Cp}_2\text{M}(\text{Ar}^{\text{iPr}_6}\text{SnH})_2$ ($\text{M} = \text{Ti, Zr, Hf}$) complexes via reaction of organodihydridostannate with group 4 metallocene dichloride highlighted the Lewis basicity of $\text{Ar}^{\text{iPr}_6}\text{SnH}$.³¹

In addition to reactivity with alkenes, workers have also examined the reactivity of low-valent group 14 element hydrides with carbonyl compounds and carbon dioxide, as conversions of CO_2

into useful chemicals are of broad interest. However, examples of Sn(II) hydrides in these processes remain scarce. In 2009, Roesky and coworkers reported hydrostannylation of CO₂ with the organotin(II) hydride, [$\{\text{HC}(\text{CMeNAr})_2\}\text{SnH}$] (Ar = 2,6-*i*Pr₂C₆H₃), as well as activated alkynes and a carbodiimide.²¹ Computational studies by Toro-Labbé and coworkers on the hydroboration of CO₂ using [$\{\text{HC}(\text{CMeNAr})_2\}\text{EH}$] (E = Si(II), Ge(II), Sn(II), and Pb(II), Ar = 2,6-*i*Pr₂C₆H₃) as catalysts demonstrated that activation energies for the catalytic cycle become lower as group 14 is descended.³⁸ However, reduction of CO₂ to formic acid and methanol by germanium hydride [$\{\text{HC}(\text{CMeNAr})_2\}\text{GeH}$] (Ar = 2,6-*i*Pr₂C₆H₃) using ammonia borane as the hydrogen source is the sole reported example among these complexes.³⁹ A recent study by Wesemann and coworkers reported the reaction of $\{\text{Ar}^{\text{iPr6}}\text{Sn}(\mu\text{-H})\}_2$ and CO₂, wherein a hydride was transferred to the carbon atom and the resulting formate anion displayed bridging coordination at two tin atoms.⁴⁰ Earlier, Jones and coworkers reported that catalytic hydroboration of carbonyl compounds and CO₂ reduction were achieved via the two-coordinated amidotin hydride [$\text{LSn}(\mu\text{-H})_2$] (L = N(Ar)(SiPr^{*i*}₃) Ar = C₆H₂{C(H)Ph₂}₂Pr^{*i*}-2,6,4) in solution, using boranes as the hydrogen source, with their turnover frequencies rivaling those of transition metal-based catalysts.⁴¹

Herein, we report the reactions of $\{\text{Ar}^{\text{iPr4}}\text{Sn}(\mu\text{-H})\}_2$ and $\{\text{Ar}^{\text{iPr6}}\text{Sn}(\mu\text{-H})\}_2$ with the molybdenum carbonyl [Mo(CO)₅(THF)], which afforded the complexes Mo(CO)₅{Sn(Ar^{*iPr6*})H}, (**1**), and Mo(CO)₅{Sn(Ar^{*iPr4*})(THF)H}, (**2**), respectively. Reactions of **1** or **2** with CO₂ were then explored. Hydrostannylation of CO₂ with **1** was formed to result in the formation of Mo(CO)₅{Sn(Ar^{*iPr6*})(κ²-O,O'-O₂CH)}, (**3**), in which a bidentate formate anion coordinated to the tin. The Lewis basic nature of Ar^{*iPr6*}SnH was shown by the isolation of the Lewis acid-base complex [(Ar^{*iPr6*})(H)Sn-Mo(CO)₅], **1**, which results from the dissociation of $\{\text{Ar}^{\text{iPr6}}\text{Sn}(\mu\text{-H})\}_2$ and its subsequent complexation with a Lewis acidic [Mo(CO)₅] moiety (Scheme 1). The catalytic potential of **1**

towards CO₂ reduction was also investigated by reacting **3** with pinacolborane in C₆D₆, where quantitative conversion of **3** to **1** and formation of a methanol equivalent was observed.

Experimental Section

General considerations

All operations were carried out under anaerobic & anhydrous conditions by using modified Schlenk techniques or in a Vacuum Atmospheres OMNI-Lab drybox under an atmosphere of dry argon or nitrogen. All solvents were dried over alumina columns and degassed prior to use.⁴² Mo(CO)₆ was used as purchased without further purification. ¹H, ¹³C, and ¹¹⁹Sn NMR spectra were collected on a Varian 600 MHz spectrometer. ¹¹B NMR spectra were collected on a 500 MHz Bruker Avance DRX spectrometer. The ¹¹B NMR data were referenced to the external standard BF₃OEt₂. The ¹¹⁹Sn NMR spectra were referenced to an external standard of SnMe₄. UV-Visible spectra were recorded in dilute hexane solutions in 3.5 mL quartz cuvettes using an Olis 17 Modernized Cary 14 UV-Vis/NIR spectrophotometer. Infrared spectra were collected on a Bruker Tensor 27 ATR-FTIR spectrometer. {Ar^{iPr4}Sn(μ-H)}₂,⁴³ {Ar^{iPr6}Sn(μ-H)}₂¹³ and [Mo(CO)₅(THF)]⁴⁴ were synthesized via literature methods.

Syntheses

Mo(CO)₅{Sn(Ar^{iPr6})H} (1). A solution of [Mo(CO)₅(THF)] (0.55 mmol, from 0.144 g Mo(CO)₆) in THF (ca. 30 mL) was added to a heavy-walled Teflon tapped Schlenk flask along with {Ar^{iPr6}SnH}₂ (0.327 g, 0.272 mmol) in THF (ca. 20 mL). Upon addition of [Mo(CO)₅(THF)], the color of the solution changed from blue to green, and then to a brownish yellow color after heating at 50 °C for 1 day. The flask was then heated at this temperature for 2 additional days. The solution was cooled to room temperature, the solvent was removed under reduced pressure and the yellow

residue was extracted with ca. 50 mL of hexanes and filtered. Storage of the solution in a ca. -30 °C freezer for 2 weeks afforded pale yellow crystals of **1** that were suitable for single crystal X-ray diffraction studies. Yield: 40.7% (0.186 g). ^1H NMR (C_6D_6 , 600 MHz, 298 K): δ 1.06 (d, 12 H, $J_{\text{HH}} = 6.7$ Hz, o- $\text{CH}(\text{CH}_3)_2$), 1.21 (d, 12 H, $J_{\text{HH}} = 7.1$ Hz, o- $\text{CH}(\text{CH}_3)_2$), 1.40 (d, 12 H, $J_{\text{HH}} = 6.7$ Hz, p- $\text{CH}(\text{CH}_3)_2$), 2.78 (hept., 2 H, $J_{\text{HH}} = 6.3$ Hz, p- $\text{CH}(\text{CH}_3)_2$), 3.09 (hept., 4 H, $J_{\text{HH}} = 6.7$ Hz, o- $\text{CH}(\text{CH}_3)_2$), 7.14-7.19 (m, 5H, m- C_6H_2 and p- C_6H_3), 7.28 (d, 2H, m- C_6H_3), 18.00 (s, 1 H, $J_{\text{Sn-H}} = 647$ Hz, Sn-H); $^{13}\text{C}\{^1\text{H}\}$ NMR (C_6D_6 , 150.6 MHz, 298 K): δ 23.46, 24.00, 26.24, 31.14, 34.77, 122.57, 128.73, 129.85, 133.56, 145.19, 147.47, 150.60, 163.10, 206.15, 212.97; $^{119}\text{Sn}\{^1\text{H}\}$ NMR (C_6D_6 , 223.6 MHz, 298 K): δ 1324 (d, $J_{\text{Sn-H}} = 668.6$ Hz). λ_{max} (ϵ): 395.8 nm ($2550 \text{ L mol}^{-1} \text{ cm}^{-1}$). IR (ν , cm^{-1}): 2073 (m), 2057 (m), 1923 (vs), 1751 (w).

$\text{Mo}(\text{CO})_5\{\text{Sn}(\text{Ar}^{\text{iPr}4})(\text{THF})\text{H}\}$ (2**).** Using a procedure similar to that used for the preparation of **1**, $[\text{Mo}(\text{CO})_5(\text{THF})]$ (0.845 mmol, from 0.223 g $\text{Mo}(\text{CO})_6$) was treated with $\{\text{Ar}^{\text{iPr}6}\text{SnH}\}_2$ (0.365 g, 0.353 mmol) to afford pale yellow crystals suitable for single crystal X-ray studies. Yield: 46.7% (0.272 g). ^1H NMR (C_6D_6 , 600 MHz, 298 K): δ 1.00 (d, 12 H, $J_{\text{HH}} = 6.8$ Hz, o- $\text{CH}(\text{CH}_3)_2$), 1.33 (d, 16 H, $J_{\text{HH}} = 6.9$ Hz, o- $\text{CH}(\text{CH}_3)_2$ overlapped with CH_2 from THF), 3.04 (hept., 2 H, $J_{\text{HH}} = 6.9$ Hz, o- $\text{CH}(\text{CH}_3)_2$), 3.43 (t, 4 H, $J_{\text{HH}} = 5.4$ Hz, THF), 7.12 (d, 4H, $J_{\text{HH}} = 7.8$ Hz, m- C_6H_3), 7.19 (t, 2H, $J_{\text{HH}} = 7.4$ Hz, p- C_6H_3), 7.23 (m, 3H, m- C_6H_3 overlapped with p- C_6H_3), 17.09 (s, 1 H, $J_{\text{Sn-H}} = 704$ Hz, Sn-H); $^{13}\text{C}\{^1\text{H}\}$ NMR (C_6D_6 , 150.6 MHz, 298 K): δ 23.32, 25.72, 26.10, 31.01, 69.22, 124.36, 127.98, 128.34, 129.98, 130.21, 136.62, 145.30, 147.26, 206.78, 212.79; $^{119}\text{Sn}\{^1\text{H}\}$ NMR (C_6D_6 , 223.6 MHz, 298 K): δ 1102.2. λ_{max} (ϵ): 402 nm ($11800 \text{ L mol}^{-1} \text{ cm}^{-1}$). IR (ν , cm^{-1}): 2059 (m), 1982 (m), 1913.63 (vs), 1795 (w).

$\text{Mo}(\text{CO})_5\{\text{Sn}(\text{Ar}^{\text{iPr}6})(\kappa^2\text{-O, O}'\text{-O}_2\text{CH})\}$ (3**).** THF (ca. 30 mL) was added to a heavy-walled Teflon tapped Schlenk flask charged with 0.435 g of **1**. Then, the solution was frozen, and the flask was

evacuated and refilled with CO₂, repeated three times. The reaction was then allowed to warm to room temperature, where the color of the solution changed from yellow to pale yellow. After stirring overnight, the solvent was removed under reduced pressure and the residue was extracted with diethyl ether. Storage of the solution in a ca. -30 °C freezer for 1 week afforded colorless crystals suitable for single crystal X-ray studies. Yield: 83.2% (0.381 g). ¹H NMR (C₆D₆, 600 MHz, 298 K): δ 1.06 (d, 12 H, J_{HH} = 6.9 Hz, o-CH(CH₃)₂), 1.27 (d, 12 H, J_{HH} = 7.1 Hz, o-CH(CH₃)₂), 1.45 (d, 12 H, J_{HH} = 7.1 Hz, p-CH(CH₃)₂), 2.85 (hept., 2 H, J_{HH} = 6.9 Hz, p-CH(CH₃)₂), 2.93 (hept., 4 H, J_{HH} = 6.8 Hz, o-CH(CH₃)₂), 7.18 (t, 1H, J_{HH} = 7.6 Hz, p-C₆H₃), 7.29 (s, 4H, m-C₆H₂), 7.30 (d, 2H, J_{HH} = 7.6 Hz, m-C₆H₃), 8.07 (s, 1 H, CO₂H); ¹³C{¹H} NMR (C₆D₆, 150.6 MHz, 298 K): δ 22.85, 24.06, 26.62, 31.44, 34.83, 121.99, 128.35, 131.33, 134.72, 145.74, 147.50, 150.33, 164.43, 174.01, 205.58, 210.21; ¹¹⁹Sn{¹H} NMR (C₆D₆, 223.6 MHz, 298 K): δ 606.1. λ_{max} (ε): 341.8 nm (shoulder, 7500 L mol⁻¹ cm⁻¹). IR (ν, cm⁻¹): 2072 (m), 1969 (w), 1934 (vs), 1605 (w), 1560 (w), 1533 (m), 1352 (m).

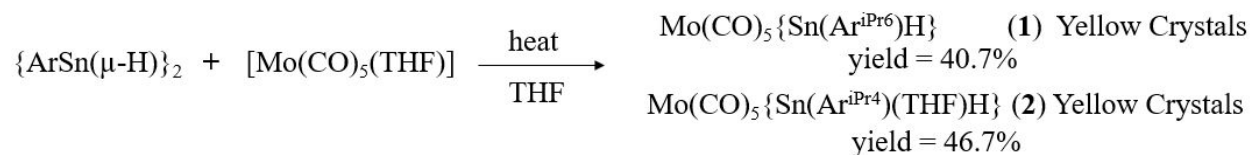
Catalytic studies. To a J Young's tube containing 20 mg of **3**, was added 0.6 mL of C₆D₆, then an excess amount of HBpin (pin = pinacolato) was added to the tube. The reactions were monitored by ¹H, and ¹¹B NMR spectroscopies. ¹H and ¹¹B NMR spectra were recorded after a brief sonication (less than 30 seconds) of the mixture. ¹H NMR spectra of the mixture solution of **3** and HBpin in C₆D₆ were recorded 5 min, 3 hours after mixing in glove box, separately. A distinct color change from almost colorless to yellow was observed upon addition of HBpin to the C₆D₆ solution of **3** (see SI).

Results and Discussion

Syntheses. Compound **1** was synthesized by gently heating 1 equivalent of {ArⁱPr₆Sn(μ-H)}₂¹⁰ THF solution with 2 equivalents of [Mo(CO)₅(THF)]³⁴ in a Schlenk flask for 3 days. (Scheme 1)

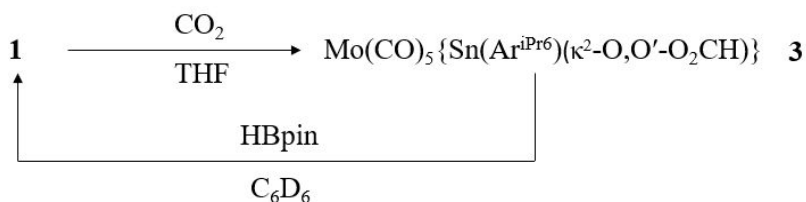
The resulting solution was extracted with hexanes, and storage of the solution in a ca. -30 °C freezer for 2 weeks afforded pale yellow crystal of **1** in moderate yield. Compound **2** was synthesized analogously using $\{\text{Ar}^{\text{iPr4}}\text{Sn}(\mu\text{-H})\}_2$.³³ Initial attempts involved either using $\text{Mo}(\text{CO})_6$ instead of $[\text{Mo}(\text{CO})_5(\text{THF})]$ or performing the above reactions at room temperature (298K) and 0 °C (273K), and ¹H NMR spectra of the crude product revealed low conversion to the product, although gentle heating to 50 °C overnight significantly improved the product yield. The moderate yield may be associated with the tendency of the $\{\text{Ar}^{\text{iPr6}}\text{Sn}(\mu\text{-H})\}_2$ or $\{\text{Ar}^{\text{iPr4}}\text{Sn}(\mu\text{-H})\}_2$, to exist in equilibrium with multiply bonded species and hydrogen.³² Also, the formation of tin clusters was reported from heating the organotin(II) hydrides in toluene, which also may account for the low overall yield.^{43, 45} Attempts in removing the coordinated THF in **2** by heating **2** at 80 °C under reduced pressure were unsuccessful.

Scheme 1. Syntheses of **1** and **2**



For the synthesis of **3** (see Scheme 2 below), a solution of **1** in THF was frozen, and the flask was evacuated under reduced pressure and refilled with CO₂, repeated three times. The reaction flask was then allowed to warm to room temperature, whereupon the color of the solution changed from yellow to pale yellow, and overnight stirring resulted in quantitative conversion of **1** to **3** based on the ¹H NMR spectrum of the crude product. Extraction with diethyl ether and storage of the solution in a ca. -30 °C freezer for 1 week afforded colorless crystals of **3** in good yield. Similar reactions were also attempted for **2**, but only a very limited reaction was observed, possibly due to lack of a coordination site at the tin atom in **2**.

Scheme 2. Reaction of **1** with CO₂, and reaction of **3** with boranes



Structures. The molecular structures of **1**, **2**, and **3** are shown in Figure 1, 2, and 3.

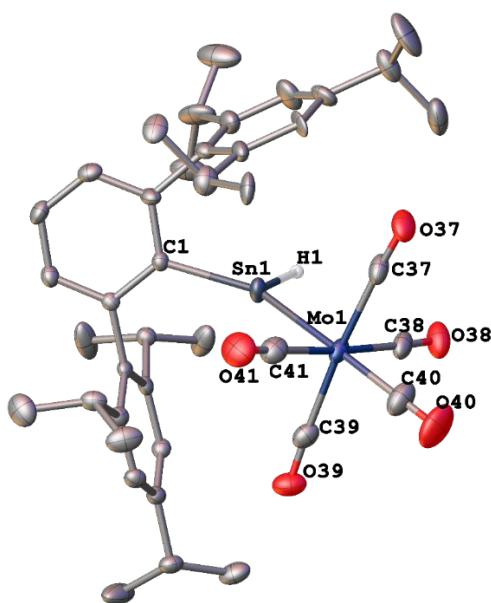


Figure 1. Solid-state molecular structure of **1** (hydrogen atoms and disorder not shown, thermal ellipsoids are shown at 50% probability). Selected bond lengths (Å) and angles (deg.): Sn(1)-C(1) 2.158(2), Sn(1)-Mo(1) 2.7157(4), Sn(1)-H(1) 1.93(2), Mo(1)-C(40) 2.018(3), Mo(1)-C(41) 2.050(3), Mo(1)-C(38) 2.050(3), Mo(1)-C(37) 2.053(3), Mo(1)-C(39) 2.053(3), C(37)-O(37) 1.143(3), C(38)-O(38) 1.139(3), C(39)-O(39) 1.143(3), C(40)-O(40) 1.135(4), C(41)-O(41) 1.140(4); C(1)-Sn(1)-Mo(1) 140.11(6), C(1)-Sn(1)-H(1) 108.3(6), Mo(1)-Sn(1)-H(1) 111.4(6).

Compound **1** features an almost trigonal planar three-coordination at the tin atom, where the sum of C(1)-Sn(1)-Mo(1), C(1)-Sn(1)-H(1), and Mo(1)-Sn(1)-H(1) angles around tin is 359.81(8)° in

1, with a terminal Sn-H bond. In contrast, compound **2** features a four-coordinate tin atom to which THF is also coordinated. In both complexes the aryltin hydride unit acts as a Lewis base via the tin lone pair, forming donor/acceptor complex with a Mo(CO)₅ unit to yield a distorted octahedral coordination geometry at molybdenum. The almost planar coordination environment generated at Sn by these ligands is consistent with a vacant p orbital located perpendicularly to the coordination plane in the structure of **1**. In **2**, the p orbital is likely to be occupied by THF but the Sn(1)-O(1) bond in the structure of **2** is not perpendicular to the coordination plane, as the O(1)-Sn(1)-H(1) angle is 62.9(19)°. The sum of the angles at tin associated with the hydride and terphenyl ligand in **2** is 359.0(19)°. In the structure of **1**, the C(1)-Sn(1)-H(1) unit is almost coplanar with that of molybdenum and the three carbonyl groups of C(38), C(40), and C(41). The C(38)-Mo(1)-Sn(1)-C(1) torsion angle is 1.2(4)°, and Sn(1)-Mo(1)-C(40) array is almost linear (176.49(8)°), whereas in the structure of **2**, the C(1)-Sn(1)-H(1) plane deviates somewhat from the molybdenum carbonyl plane, and the C(32)-Mo(1)-Sn(1)-C(1) torsion angle is 17(2)°. The Sn-H distance in **1** is 1.93(2) Å, and 1.82(6) Å for **2**. These values may be compared to that of the terminal Sn-H bond, 1.74(3) Å, in [$\{HC(CMeNAr)_2\}SnH$] reported by Roesky and coworkers,¹⁴ and Sn-H bonds in Cp₂M(Ar^{iPr6}SnH)₂ (M = Ti, Zr, Hf) complexes reported by Wesemann and coworkers, which range from 1.69(2) to 1.776(18) Å.³¹ The Mo-C bond lengths in **1** and **2**, Mo(1)-C(40) for **1** and Mo(1)-C(35) for **2**, which are trans to Ar^{iPr6}SnH ligand, are 2.018(3) Å for **1**, 1.999(7) Å for **2**, respectively, showing little variation. In the structure of **1**, the average Mo-C bond length of other four carbonyls is 2.052(3) Å, suggesting stronger pi-back bonding for Mo(1)-C(40) bond, where in the structure of **2**, the average bond length of other four carbonyls is 2.037(6) Å. This is likely a result of the increased electron density at molybdenum due to the favorable sigma-donor properties of the Ar^{iPr6}SnH ligand and its relatively weak pi-acceptor character.⁴⁶ The Sn(1)-Mo(1) bond length is

2.716(4) Å in **1**, and 2.756(6) Å in **2**, which are similar to the Sn-Mo bond length (2.784(17) Å) in $(\text{CO})_5\text{MoSn}(\mu_2\text{-O}^t\text{Bu})_3\text{Ce}(\text{O}^t\text{Bu})_3$ reported by Mathur and coworkers.⁴⁷ The sum of the covalent radii of Mo and Sn is 2.93(5) Å,⁴⁸ which is longer than Sn-Mo single bonds in **1** and **2**. The Sn-Mo triple bond in $\text{Ar}^{\text{iPr}_6}\text{SnMo}(\eta^5\text{-C}_5\text{H}_5)(\text{CO})_2$ results from metathetical exchange reaction between the distannyne, $\text{Ar}^{\text{iPr}_6}\text{Sn}=\text{SnAr}^{\text{iPr}_6}$, and $(\text{CO})_2(\eta^5\text{-C}_5\text{H}_5)\text{Mo}=\text{Mo}(\eta^5\text{-C}_5\text{H}_5)(\text{CO})_2$, is 2.4691(7) Å.⁴⁹

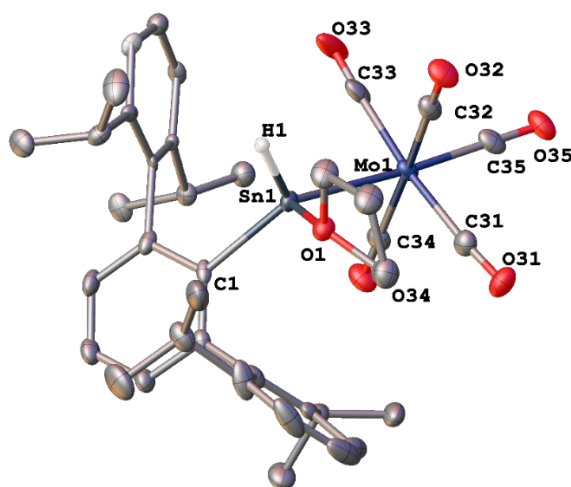


Figure 2. Solid-state molecular structure of **2** (hydrogen atoms and disorder are not shown, thermal ellipsoids are shown at 30% probability). Selected bond lengths (Å) and angles (deg.): Sn(1)-C(1) 2.198(5), Sn(1)-Mo(1) 2.7563(6), Sn(1)-H(1) 1.82(6), Mo(1)-C(35) 1.999(6), Mo(1)-C(31) 2.024(6), Mo(1)-C(32) 2.025(6), Mo(1)-C(33) 2.053(6), Mo(1)-C(34) 2.046(6), C(31)-O(31) 1.149(6), C(32)-O(32) 1.157(6), C(33)-O(33) 1.147(7), C(34)-O(34) 1.146(6), C(35)-O(35) 1.153(6); C(1)-Sn(1)-Mo(1) 134.31(11), C(1)-Sn(1)-H(1) 105.9(19), Mo(1)-Sn(1)-H(1) 118.8(19), O(1)-Sn(1)-H(1) 62.9(19).

The molecular structure of **3** features a four-coordinate tin atom that is coordinated by a bidentate formate ligand, a terphenyl group, and $\text{Mo}(\text{CO})_5$ moiety. Complex **3** possesses an internal mirror plane incorporating the C(1)-Sn(1)-Mo(1) array. The formate ligand is symmetrically bound to the tin atom, and the two Sn-O bonds being equal, 2.2228(12) Å, underlying the resonance structure of formate anion. These may be compared to the Sn-O bonds in $\text{LSn}(\kappa^2\text{-O},\text{O}'\text{-O}_2\text{CH})$ ($\text{L}=\text{-}$

$N(\text{Ar})(\text{SiPr}^i_3)$ Ar = $\text{C}_6\text{H}_2\{\text{C}(\text{H})\text{Ph}_2\}_2\text{Pr}^i$ -2,6,4) reported by Jones and coworkers are 2.353(2), and 2.333(2), respectively.⁴¹ The Mo(1)-C(21) bond, 2.011(3) Å in **3** is slightly shortened in comparison to the Mo(1)-C(40), 2.018(3) Å, bond in the structure of **1**, suggesting similar sigma-donor properties of the $\text{Ar}^{\text{iPr}^6}\text{Sn}(\kappa^2\text{-O},\text{O}'\text{-O}_2\text{CH})$ moiety and $\text{Ar}^{\text{iPr}^6}\text{SnH}$.

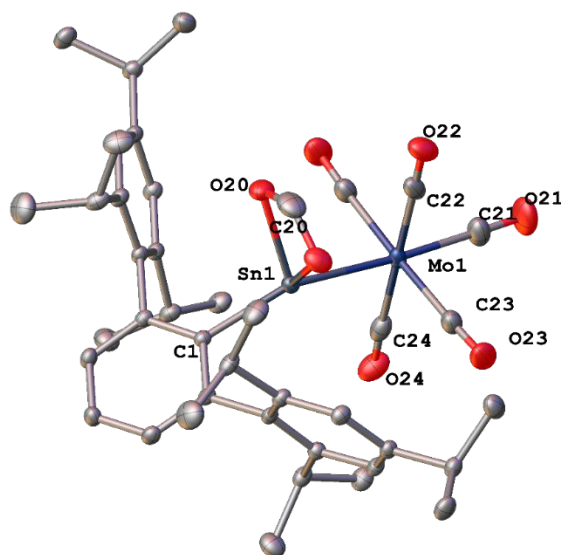


Figure 3. Solid-state molecular structure of **3** (hydrogen atoms and disorder are not shown, thermal ellipsoids are shown at 50% probability). Selected bond lengths (Å) and angles (deg.): Sn(1)-Mo(1) 2.158(2), Sn(1)-Mo(1) 2.723(3), Mo(1)-C(21) 2.011(3), Mo(1)-C(22) 2.036(3), Mo(1)-C(23) 2.054(3), Mo(1)-C(24) 2.062(3), C(21)-O(21) 1.140(4), C(22)-O(22) 1.147(3), C(23)-O(23) 1.138(2), C(24)-O(24) 1.142(3); C(1)-Sn(1)-Mo(1) 152.54(5), C(1)-Sn(1)-O(20) 98.18(6).

NMR Spectroscopy. The solution ^1H NMR spectra of **1**, **2**, and **3** displayed signals corresponding to the Ar^{iPr^4} or Ar^{iPr^6} ligands with diastereotopic isopropyl methyl groups and septet methine signals, and showed little difference from those reported for $\{\text{Ar}^{\text{iPr}^4}\text{Sn}(\mu\text{-H})\}_2$ or $\{\text{Ar}^{\text{iPr}^6}\text{Sn}(\mu\text{-H})\}_2$.^{13, 43} The Sn-H signal is however observed at $\delta = 18.03$ ppm for **1**, and at $\delta = 17.09$ ppm for **2**, which are much further downfield than the Sn-H signal at $\delta = 7.87$ ppm for $\{\text{Ar}^{\text{iPr}^6}\text{Sn}(\mu\text{-H})\}_2$, and $\delta = 9.13$ ppm for $\{\text{Ar}^{\text{iPr}^4}\text{Sn}(\mu\text{-H})\}_2$. The downfield shift of the signals can be attributed to the

terminal nature of the Sn-H bonds in each compound, and the coordination of the transition metal to the tin atom.⁴⁶ Compared to **1**, the Sn-H signal in **2** is shifted slightly upfield, possibly as a result of the THF coordination and consequent increased electron density at the tin atom in **2**. The calculated ¹H NMR chemical shift of the Sn-H hydrogen of the hypothetical monomeric unit of {Ar^{iPr6}Sn(μ-H)}₂ is δ=25.4 ppm,³⁴ and coordination of transition metal carbonyl moiety should result in further a downfield shift⁴⁶ of the Sn-H signal which contradicts to the experimentally observed shifts of the hydrogens for Sn-H in **1** and **2**. The Sn-H chemical shifts of **1** and **2** are in good agreement with that seen for the hydride-bridged tin(II) species, {LSn(μ-H)}₂ (L=N(Ar)(SiPr₃) Ar = C₆H₂{C(H)Ph₂}₂Prⁱ-2,6,4), which dissociated to monomers when dissolved in an aromatic solvent, as reported by Jones and coworkers (Sn-H δ=17.20 ppm at 298 K, broad Sn-H at δ=19.20 ppm at 313K),¹⁹ and δ=19.4 ppm observed for a hydrogen-substituted stannylene complex, Cp^{*}(iPr₃P)(H)Os=SnH(trip) (trip = 2,4,6-triisopropylphenyl), of Tilley and coworkers.⁵⁰ ^{117/119}Sn satellites were also observed for the Sn-H signal with a coupling constant of 647 Hz for **1** and 704 Hz for **2**. The ¹H NMR signal of the formate hydrogen in **3** was observed at downfield region, 8.07 ppm. The ¹³C{¹H} NMR spectra of **1**, **2** and **3** displayed two distinct chemical shifts for the carbonyl resonances in an approximate 1:4 ratio, which is consistent with their structures data for **1**, **2**, and **3** (see above), while ¹³C-^{117/119}Sn coupling was not observed. The carbonyl resonances suggest that the rotations around Mo-Sn bond in **1** and **2** are not restricted, and thus the monomeric unit, Ar^{iPr6}SnH, is a better σ-donor than it is a π-acceptor despite the presence of an empty p-orbital on the Sn atom, which is further demonstrated in calculations (vide infra).

The ¹¹⁹Sn{¹H} NMR spectra of **1**, **2**, and **3** were recorded in C₆D₆ and referenced to the external standard SnMe₄ in CDCl₃. The ¹¹⁹Sn signal of **1** appeared at δ = 1324 ppm, which is slightly further downfield than the range of three-coordinated tin-transition metal complexes (673-1231 ppm).⁵¹⁻

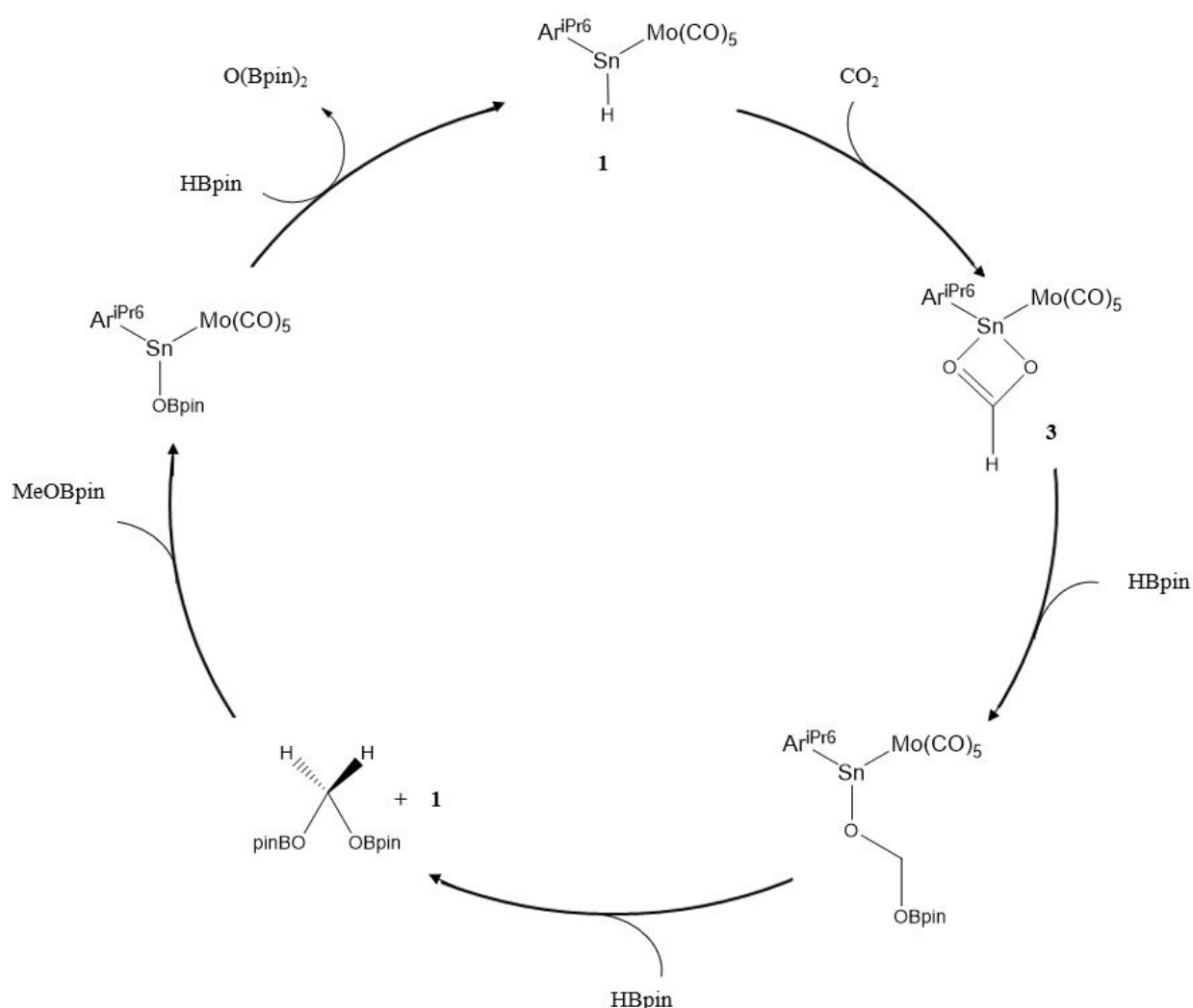
⁵⁶ The ¹H-coupled ¹¹⁹Sn NMR spectrum of **1** displayed a doublet signal ($J_{\text{Sn-H}} = 649$ Hz) which matches both the ¹H NMR spectrum and is consistent with molecular structure of **1**. The ¹¹⁹Sn spectrum of **2** displayed one signal at $\delta = 1102$ ppm, which is slightly more upfield than that of **1**, likely a result of the increased electron density due to the coordinated THF molecule. Both the ¹¹⁹Sn{¹H} NMR spectra of **1** and **2** agree well with the ¹¹⁹Sn NMR chemical shift of Cp₂M(Ar^{iPr6}SnH)₂ (M = Ti, Zr, Hf) complexes reported by Wesemann and coworkers, which ranged from 1060 to 1250 ppm.³¹

The ¹¹⁹Sn NMR signal of **3** appeared at $\delta = 606$ ppm, which is further downfield than those of other divalent or tetravalent tin formates⁵⁷, as reported by Roesky and coworkers for [$\{\text{HC}(\text{CMeNAr})_2\} \text{Sn-OC}(\text{O})\text{H}$] (Ar = 2,6-iPr₂C₆H₃) at -360 ppm.²¹ Jones and coworkers reported the ¹¹⁹Sn{¹H} NMR chemical shift of LSn ($\kappa^2\text{-O,O'-O}_2\text{CH}$) (L= $\text{-N}(\text{Ar})(\text{SiPr}^i_3)$ Ar = C₆H₂{C(H)Ph₂}₂Prⁱ-2,6,4) at -134 ppm, where the formate has the same bidentate coordination as **3**.⁴¹ The ¹¹⁹Sn{¹H} NMR chemical shift of Ar^{iPr6}Sn(H)OC(H)OSnAr^{iPr6} was reported at 113.4 ppm by Wesemann and coworkers.⁴⁰ The downfield shift of ¹¹⁹Sn NMR of **3** is likely due to the coordination of [Mo(CO)₅] fragment at the tin atom⁴⁶, compared to those reported for organotin formates.⁵⁷

We investigated the catalytic potential of **1** towards hydrogenation of CO₂, which is enabled at the tin atom in **1** by its coordinative unsaturation. Initial attempts using dihydrogen gas or NaH as the hydrogen source in the regeneration of **1** were unsuccessful, however, using HBpin (pin = pinacolato) as the hydrogen source resulted in quantitative conversion from **3** to **1**. The ¹H NMR spectrum of a mixture of **3** and HBpin showed signals attributable to the unreacted species, **3** and HBpin, 5 min after mixing in glove box. Then, after 3 hours at room temperature, the ¹H NMR spectrum indicated complete conversion of **3** to **1**, as evidenced by the disappearance of the 8.07

ppm signal of the formate in **3**, and the appearance of a new signal which corresponded to the Sn-H hydrogen of **1** at 18.07 ppm emerged. (Scheme 2) ^{11}B NMR spectroscopy of the reaction between **3** and pinacolborane showed two additional signals apart from the excess amount of HBpin, which are attributed to $(\text{pinB})_2\text{O}$, and $\text{MeOBpin}^{58, 59}$, which is considered as a methanol equivalent (see Scheme 3).

Scheme 3. Proposed cycle for the reduction of CO_2 , catalyzed by **1**



IR spectroscopy. Compounds **1** and **2** displayed three ν_{CO} stretching bands and one Sn-H stretching band in their FT-IR spectra. The weak absorption at 1752 (w) cm^{-1} for **1** and 1795 (w)

cm⁻¹ for **2** were assigned to the Sn-H stretching mode, while the other three bands at, 2074 (m), 2058 (m), and 1924 (vs) cm⁻¹ for **1**, 2059 (m), or 1982 (m), and 1913 (vs) cm⁻¹ for **2** are attributed to the three CO stretching bands. This three-band pattern is considered to be characteristic of a [LM(CO)₅] species.⁶⁰ The ν_{CO} stretching frequencies of **1** are lower than those of [Mo(CO)₅PPh₃] and other molybdenum phosphine complexes as reported by Cotton and coworkers,⁶¹ which suggests that the Ar^{iPr₆}SnH unit is a weaker π -acceptor than a phosphine ligand. The Sn-H stretching frequencies of **1** and **2** differ from those of the previously reported bridged-hydride Sn(II) species, {Ar^{iPr₆}Sn(μ -H)}₂ ($\nu_{\text{Sn-H}}$ =1828, 1771 cm⁻¹), which are due to the asymmetric isomeric {Ar^{iPr₆}SnSn(H)₂Ar^{iPr₆}}.^{13, 16} The Sn-H stretching frequencies of the terminal Sn-H bonds were reported to be [{HC(CMeNAr)₂}SnH] (Ar = 2,6-iPr₂C₆H₃) $\nu_{\text{Sn-H}}$ = 1849 cm⁻¹,¹⁴ and [{2,6-iPr₂C₆H₃NCMe}₂C₆H₃SnH] $\nu_{\text{Sn-H}}$ = 1826 cm⁻¹.¹⁵ The stretching frequency, however is in close agreement with those of Cp₂M(Ar^{iPr₆}SnH)₂ (M = Ti, Zr, Hf) complexes, from 1741 to 1749 cm⁻¹,³¹ and calculated stretching frequency for the Ar^{iPr₄}SnH monomer, 1734 cm⁻¹.¹⁶

The IR spectrum of compound **3** displayed CO stretching bands that are similar to those of **1** and **2**. The Sn-H stretching band at 1752 cm⁻¹ is no longer apparent. However, another absorbance appeared at 1533 cm⁻¹ which arises from the carbonyl group of the formate, HCO₂⁻. The carbonyl stretching frequency of [{HC(CMeNAr)₂}Sn-OC(O)H] (Ar = 2,6-iPr₂C₆H₃) was reported to be 1641 cm⁻¹.²¹ Jones and coworkers reported carbonyl stretching frequency of LSn(κ^2 -O,O'-O₂CH)} (L=N(Ar)(SiPr₃) Ar = C₆H₂{C(H)Ph₂}₂Prⁱ-2,6,4) at 1549 cm⁻¹,⁴¹ which agrees well with the carbonyl stretching frequency of the bidentate formate in **3**.

Computational Analysis.

The structure of **1** was subjected to refinement at the DFT level of theory (B3LYP, see computational details). Overall, the calculated and experimental bond angles of compound **1** agree

well, and the slight deviations between the experimental and calculated bond angles could be a result of intermolecular interactions for the former in the solid state. The calculated bond length of Sn-Mo bond is 2.723 Å, which is in close agreement to that observed in the crystal structure of **1**, 2.7157(4) Å. However, the calculated bond length of Sn-H bond, 1.750 Å, deviates from the experimentally observed, 1.93(2) Å.

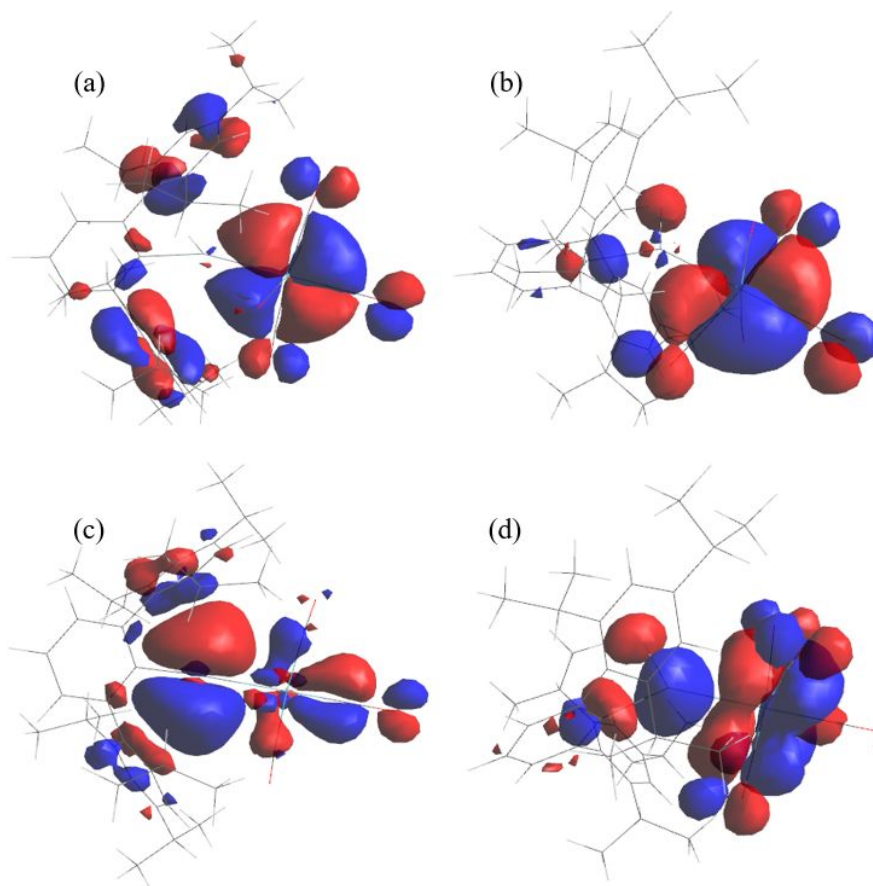


Figure 4. (a) HOMO-1 (-5.801 eV), (b) HOMO (-5.655 eV), (c) LUMO (-3.115 eV), (d) LUMO+1 (-2.319 eV)

Analysis of the frontier orbitals (Figure 4) of **1** reveals no significant π -back bonding between molybdenum and tin, despite having an available p-orbital at the tin. The major component of the HOMO is located on molybdenum, and illustrating pi-back bonding between Mo(1)-C(40), while

the LUMO is located largely on tin, where a p-orbital is centered at tin, lying perpendicular to the C(1)-Sn(1)-H(1) plane. The LUMO indicates a coordinative unsaturation at tin, likely resulted from steric shielding exerted by the terphenyl ligand. For simplicity, a phenyl group has been used in place of Ar^{iPr6} group to calculate vibrational frequencies of **1**. The terminal Sn-H bond is calculated to have a stretching frequency of 1762 cm⁻¹, which is in close agreement with what was observed experimentally, 1752 cm⁻¹.

Conclusion

We have shown that reactions of aryltin(II) hydrides {Ar^{iPr4}Sn(μ-H)}₂ or {Ar^{iPr6}Sn(μ-H)}₂ with two equivalents of the group 6 carbonyls, [Mo(CO)₅(THF)], yield either a stable, monomeric, three coordinate, divalent tin hydride transition metal complex, Mo(CO)₅{Sn(Ar^{iPr6})H}, (**1**), or a four coordinate tin hydride species Mo(CO)₅{Sn(Ar^{iPr4})(THF)H}, (**2**). Hydrostannylation of carbon dioxide by **1** afforded the complex, Mo(CO)₅{Sn(Ar^{iPr6})(κ²-O,O'-O₂CH)}, (**3**), incorporating a bidentate formate anion coordinated to the tin atom. The catalytic potential of **1** was investigated by reaction of **3** with pinacolborane in C₆D₆, where **1** was generated in nearly quantitative yield. The complexes were characterized by single crystal X-ray diffraction, UV-Visible, IR, and multinuclear NMR spectroscopy. The isolation of **1** and **2** gives supporting evidence to the existence of monomeric form of {Ar^{iPr4}Sn(μ-H)}₂ and {Ar^{iPr6}Sn(μ-H)}₂ in solution by its trapping as a donor ligand in complexation to [Mo(CO)₅] moiety to afford an acid-base complex. Regeneration of **1** from **3** via reaction with pinacolborane as a hydrogen source suggests the promising catalytic potential of **1** in the hydrogenation of CO₂.

Electronic Supplementary Information (ESI) available. CCDC 2085598 (CIF), 2085599 (CIF), 2085600 (CIF), and Optimized Cartesian coordinates (XYZ) see doi/10.1039/d1dtxxxx

Conflicts of interest

There are no conflicts to declare.

Acknowledgements

We are grateful for the Office of Basic Energy Sciences, U.S. Department of Energy (Grant DE-FG02-07ER4675) and the dual-source X-ray diffractometer (Grant 0840444) for financial support. We acknowledge Dr. Louis M. Longaker for his early contribution to this work.

AUTHOR INFORMATION

Corresponding Author

Philip P. Power – *Department of Chemistry, University of California, Davis, California 95616, United States;*

orcid.org/0000-0002-6262-3209; Email: pppower@ucdavis.edu

Authors

Qihao Zhu – *Department of Chemistry, University of California, Davis, California 95616, United States;*

orcid.org/0000-0002-5566-4491

James C. Fetting – *Department of Chemistry, University of California, Davis, California 95616, United States;*

orcid.org/0000-0002-6428-4909

Notes and References

1. R. P. Attrill, M. A. Blower, K. R. Mulholland, J. K. Roberts, J. E. Richardson, M. J. Teasdale and A. Wanders, *Org. Process Res. Dev.*, 2000, **4**, 98-101.
2. A. P. Dobbs and F. K. I. Chio, in *Comprehensive Organic Synthesis II (Second Edition)*, ed. P. Knochel, Elsevier, Amsterdam, 2014, pp. 964-998.
3. V. Caprio, in *Comprehensive Organic Functional Group Transformations II*, eds. A. R. Katritzky and R. J. K. Taylor, Elsevier, Oxford, 2005, pp. 135-214.
4. G. F. Bradley and S. R. Stobart, *J. Chem. Soc., Dalton Trans.*, 1974, 264-269.
5. T. Saegusa, Y. Ito, S. Kobayashi and K. Hirota, *J. Am. Chem. Soc.*, 1967, **89**, 2240-2241.
6. C. D. Beard and J. C. Craig, *J. Am. Chem. Soc.*, 1974, **96**, 7950-7954.
7. R. D. Adams, F. A. Cotton, W. R. Cullen, D. L. Hunter and L. Mihichuk, *Inorg. Chem.*, 1975, **14**, 1395-1399.
8. G. Manuel, G. Bertrand and P. Mazerolles, *J. Organomet. Chem.*, 1978, **146**, 7-16.
9. C. Walling, J. H. Cooley, A. A. Ponaras and E. J. Racah, *J. Am. Chem. Soc.*, 1966, **88**, 5361-5363.
10. T. J. Hadlington, M. Driess and C. Jones, *Chem. Soc. Rev.*, 2018, **47**, 4176-4197.
11. E. Rivard and P. P. Power, *Dalton Trans.*, 2008, 4336-4343.

12. S. Aldridge and A. J. Downs, *Chem. Rev.*, 2001, **101**, 3305-3366.
13. B. E. Eichler and P. P. Power, *J. Am. Chem. Soc.*, 2000, **122**, 8785-8786.
14. L. W. Pineda, V. Jancik, K. Starke, R. B. Oswald and H. W. Roesky, *Angew. Chem. Int. Ed.*, 2006, **45**, 2602-2605.
15. S. Khan, P. P. Samuel, R. Michel, J. M. Dieterich, R. A. Mata, J.-P. Demers, A. Lange, H. W. Roesky and D. Stalke, *Chem. Commun.*, 2012, **48**, 4890-4892.
16. E. Rivard, R. C. Fischer, R. Wolf, Y. Peng, W. A. Merrill, N. D. Schley, Z. Zhu, L. Pu, J. C. Fettinger, S. J. Teat, I. Nowik, R. H. Herber, N. Takagi, S. Nagase and P. P. Power, *J. Am. Chem. Soc.*, 2007, **129**, 16197-16208.
17. A. F. Richards, A. D. Phillips, M. M. Olmstead and P. P. Power, *J. Am. Chem. Soc.*, 2003, **125**, 3204-3205.
18. J. Schneider, C. P. Sindlinger, K. Eichele, H. Schubert and L. Wesemann, *J. Am. Chem. Soc.*, 2017, **139**, 6542-6545.
19. T. J. Hadlington, M. Hermann, J. Li, G. Frenking and C. Jones, *Angew. Chem. Int. Ed.*, 2013, **52**, 10199-10203.
20. J. D. Queen, J. C. Fettinger and P. P. Power, *Chem. Commun.*, 2019, **55**, 10285-10287.
21. A. Jana, H. W. Roesky, C. Schulzke and A. Döring, *Angew. Chem. Int. Ed.*, 2009, **48**, 1106-1109.
22. A. Jana, H. W. Roesky, C. Schulzke and P. P. Samuel, *Organometallics*, 2010, **29**, 4837-4841.
23. R. Rodriguez, D. Gau, Y. Contie, T. Kato, N. Saffon-Merceron and A. Baceiredo, *Angew. Chem. Int. Ed.*, 2011, **50**, 11492-11495.
24. T. J. Hadlington, M. Hermann, G. Frenking and C. Jones, *Chem. Sci.*, 2015, **6**, 7249-7257.
25. P. P. Power, *Nature*, 2010, **463**, 171-177.
26. G. D. Frey, V. Lavallo, B. Donnadiou, W. W. Schoeller and G. Bertrand, *Science*, 2007, **316**, 439.
27. M. M. D. Roy, S. Fujimori, M. J. Ferguson, R. McDonald, N. Tokitoh and E. Rivard, *Chem. Eur. J.*, 2018, **24**, 14392-14399.
28. S. M. I. Al-Rafia, A. C. Malcolm, S. K. Liew, M. J. Ferguson and E. Rivard, *J. Am. Chem. Soc.*, 2011, **133**, 777-779.
29. T. P. Dhungana, H. Hashimoto and H. Tobita, *Dalton Trans.*, 2017, **46**, 8167-8179.
30. K. Inomata, T. Watanabe, Y. Miyazaki and H. Tobita, *J. Am. Chem. Soc.*, 2015, **137**, 11935-11937.
31. J.-J. Maudrich, M. Widemann, F. Diab, R. H. Kern, P. Sirsch, C. P. Sindlinger, H. Schubert and L. Wesemann, *Chem. Eur. J.*, 2019, **25**, 16081-16087.
32. S. Wang, T. J. Sherbow, L. A. Berben and P. P. Power, *J. Am. Chem. Soc.*, 2018, **140**, 590-593.
33. S. Wang, M. L. McCrea-Hendrick, C. M. Weinstein, C. A. Caputo, E. Hoppe, J. C. Fettinger, M. M. Olmstead and P. P. Power, *J. Am. Chem. Soc.*, 2017, **139**, 6596-6604.
34. J. Vicha, R. Marek and M. Straka, *Inorg. Chem.*, 2016, **55**, 10302-10309.
35. C. P. Sindlinger and L. Wesemann, *Chem. Sci.*, 2014, **5**, 2739-2746.
36. C. P. Sindlinger, A. Stasch, H. F. Bettinger and L. Wesemann, *Chem. Sci.*, 2015, **6**, 4737-4751.
37. C. P. Sindlinger, W. Grahneis, F. S. W. Aicher and L. Wesemann, *Chem. Eur. J.*, 2016, **22**, 7554-7566.
38. N. Villegas-Escobar, H. F. Schaefer and A. Toro-Labbé, *J. Phys. Chem. A*, 2020, **124**, 1121-1133.
39. A. Jana, G. Tavčar, H. W. Roesky and M. John, *Dalton Trans.*, 2010, **39**, 9487-9489.
40. S. Weiß, M. Widemann, K. Eichele, H. Schubert and L. Wesemann, *Dalton Trans.*, 2021, **50**, 4952-4958.
41. T. J. Hadlington, C. E. Kefalidis, L. Maron and C. Jones, *ACS Catalysis*, 2017, **7**, 1853-1859.
42. A. B. Pangborn, M. A. Giardello, R. H. Grubbs, R. K. Rosen and F. J. Timmers, *Organometallics*, 1996, **15**, 1518-1520.
43. E. Rivard, J. Steiner, J. C. Fettinger, J. R. Giuliani, M. P. Augustine and P. P. Power, *Chem. Commun.*, 2007, 4919-4921.
44. M. J. Boylan, P. S. Braterman and A. Fullarton, *J. Organomet. Chem.*, 1971, **31**, C29-C30.
45. A. F. Richards, B. E. Eichler, M. Brynda, M. M. Olmstead and P. P. Power, *Angew. Chem. Int. Ed.*, 2005, **44**, 2546-2549.

46. W. Petz, *Chem. Rev.*, 1986, **86**, 1019-1047.
 47. J. Schläfer, S. Stucky, W. Tyrra and S. Mathur, *Inorg. Chem.*, 2013, **52**, 4002-4010.
 48. P. Pyykkö and M. Atsumi, *Chem. Eur. J.*, 2009, **15**, 186-197.
 49. J. D. Queen, A. C. Phung, C. A. Caputo, J. C. Fettinger and P. P. Power, *J. Am. Chem. Soc.*, 2020, **142**, 2233-2237.
 50. P. G. Hayes, C. W. Gribble, R. Waterman and T. D. Tilley, *J. Am. Chem. Soc.*, 2009, **131**, 4606-4607.
 51. M. Weidenbruch, A. Stilter, J. Schlaefke, K. Peters and H. G. v. Schnering, *J. Organomet. Chem.*, 1995, **501**, 67-70.
 52. M. Weidenbruch, A. Stilter, K. Peters and H. G. von Schnering, *Z. Anorg. Allg. Chem.*, 1996, **622**, 534-538.
 53. M. Weidenbruch, A. Stilter, W. Saak, K. Peters and H. G. von Schnering, *J. Organomet. Chem.*, 1998, **560**, 125-129.
 54. J. J. Schneider, N. Czap, D. Bläser and R. Boese, *J. Am. Chem. Soc.*, 1999, **121**, 1409-1410.
 55. J. Bareš, P. Richard, P. Meunier, N. Pirio, Z. Padělková, Z. Černošek, I. Císařová and A. Růžička, *Organometallics*, 2009, **28**, 3105-3108.
 56. J. J. Schneider, N. Czap, D. Bläser, R. Boese, J. Ensling, P. Gülich and C. Janiak, *Chem. Eur. J.*, 2000, **6**, 468-474.
 57. B. D. Ellis, T. M. Atkins, Y. Peng, A. D. Sutton, J. C. Gordon and P. P. Power, *Dalton Trans.*, 2010, **39**, 10659-10663.
 58. Y. C. A. Sokolovicz, O. Nieto Faza, D. Specklin, B. Jacques, C. S. López, J. H. Z. dos Santos, H. S. Schrekker and S. Dagorne, *Catal. Sci. Technol.*, 2020, **10**, 2407-2414.
 59. X. Cao, W. Wang, K. Lu, W. Yao, F. Xue and M. Ma, *Dalton Trans.*, 2020, **49**, 2776-2780.
 60. P. Kircher, G. Huttner, K. Heinze, B. Schiemenz, L. Zsolnai, M. Büchner and A. Driess, *Eur. J. Inorg. Chem.*, 1998, **1998**, 703-720.
 61. F. A. Cotton, D. J. Darensbourg and W. H. Ilsley, *Inorg. Chem.*, 1981, **20**, 578-583.
-